A Robust Control Approach for Maneuvering a Flexible Spacecraft

Yoon-Gyeoung Sung*, Jea-Won Lee
School of Mechanical Engineering, Yeungnam University
Hunmo Kim
School of Mechanical Engineering, Sungkyunkwan University

In the paper, a robust control mechanism is presented to maneuver a flexible spacecraft with the deflection reduction during large slewing operation at the same time. For deflection reduction and maneuvering of the flexible spacecraft, a control mechanism is developed with the application of stochastic optimal sliding-mode control, a linear tracking model and input shaping technique. A start-coast-stop maneuver is employed as a slewing strategy. It is shown that the control mechanism with the strategic maneuver results in better performance and is more efficient than rigid-body-like maneuver, by applying to the Spacecraft Control Laboratory Experiment (SCOLE) system in a space environment.

Key Words : Optimal Sliding-Mode Control, Input Shaping Technique, Robust Control, Flexible Spacecraft

1. Introduction

In the future generation of flexible spacecraft, the control system design will be a challenging problem because of their special dynamic characteristics which include a large number of significant elastic modes with very small inherent damping, inaccuracies in the knowledge of system parameters, nonlinear effects and stringent maneuver accuracy. The control methods are related with a multi-input, multi-output (MIMO) configuration. As a result, it is natural to use an optimal formulation to design a controller. However, stringent stability and robustness are required due to space operations with minimum energy consumption. In order to satisfy these requirements, many algorithms have been proposed by employing optimal control, adaptive control, robust control, etc.

Recently, sliding-mode control has been used extensively in robotics (Slotine, 1985), in which state information is readily available. Slotine proposed the boundary layer concept to reduce the chattering problem by introducing a linear function within the switching region. In the application of SMC to flexible structures, Mostafa and Öz (1989) investigated a switching mechanism, stability, interaction with unmodeled dynamics, and the chattering problem with general nonlinear systems. They determined that the chattering issue is not the main obstacle to the application of SMC, but the effect of truncated modes may cause instability in a nonlinear system, in contrast to a linear system, due to control spillover alone. Young and Özguner (1993) combined SMC with a frequency weighted optimal formulation (Gupta, 1980) to reduce the chattering. Sinha and Miller (1995) proposed an optimal SMC with Kalman filter to reject stochastic broadband torque disturbances. However, an estimator-based tracking SMC has not been adequately addressed. Sung (1997) developed a sto-

* Corresponding Author,
E-mail : sungyg@yu.ac.kr
TEL : *+82-53-810-3536* ; ***FAX*** : *+82-53-813-3703*
School of Mechanical Engineering, Yeungnam University, 241-1, Dae-dong, Kyungsan, Kyungbook 712-749, Korea. (Manuscript **Received** December 10, 1998; **Revised** November 23, 2000)

chastic optimal sliding-mode controller (SOSMC) in conjunction with Kalman filtering to control the oscillatory deflection of large flexible structures. He investigated closed-loop dynamics and globally asymptotic stability of the SOSMC algorithm. Using a two-mass-spring-damper system, Sung (1999b) investigated an energy efficient control approach by combining SMC with the input shaping technique. It was illustrated that a synthesized trajectory with a combination of low-frequency mode and rigid-body mode results in better performance than the traditional rigid-body trajectory alone.

An objective pursued by the paper is to reduce residual deflection and to largely slew a flexible spacecraft by fabricating the SOSMC law, an elastic tracking model and the input shaping technique. The paper is organized as follows. In the next section, the dynamic equations of a flexible spacecraft are reviewed. Then, a model reduction is presented for efficient computation and deflection control. In the following section, matrix partition approach is used under the assumption of measurable rigid-body states to formulate an elastic tracking model in order to avoid the control spillover. Lastly, a start-coast-stop maneuver is proposed as a slewing strategy. In the numerical simulation, the proposed control mechanism demonstrates the control efficacy and satisfies the stringent final antenna error below 0.02° within the short period of time for the control objective of the SCOLE.

2. Dynamics of a Flexible Spacecraft

The spacecraft consists of a shuttle carrying an antenna connected to the shuttle by means of a mast, as shown in Fig. 1. The shuttle is assumed to be rigid and the mast and antenna are deformable. The motion of the spacecraft is referred to a given reference frame $x_0y_0z_0$ embedded in the rigid shuttle. The reference frame has six degrees of freedom, three rigid-body rotations and three rigid-body translations. A set of simultaneous nonlinear ordinary differential equations can be found in reference (Meirovitch and Quinn, 1987b). They presented a perturbation approach which consists of separating the equations into a set of equations for the rigid-body motions, representing zero-order effects, and a set of equations for the small elastic motions and deviations from the rigid-body motions, representing first-order effects. Their approach permits a maneuver strategy that is independent on the deflection control. The resulting perturbation equations are summarized in the following.

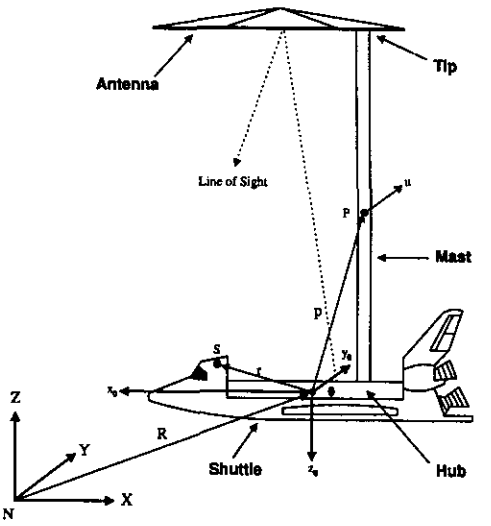

Fig. 1 Spacecraft control laboratory experiment configuration

The zero-order equations of motion, which govern the structure as if it were rigid, are shown to have the expressions

$$m\ddot{R}_0+C_0^T\tilde{S}_0\dot{\omega}_0+\frac{Gm_e}{\|R_0\|^3}[mR_0 +(I-2\hat{R}_0\hat{R}_0^T)C_0^TS_0]=C_0^TF_0 \quad (1)$$

$$\tilde{S}_0^TC_0\ddot{R}_0+\frac{Gm_e}{\|R_0\|^3}\tilde{S}_0^TC_0R_0+I_0\dot{\omega}_0+\tilde{\omega}_0^TI_0\omega_0 =M_0 \quad (2)$$

where m_e is the mass of the earth and G is the universal gravitational constant. F_0 and M_0 are the zero-order perturbed control force and moment vectors in that order. m, m_S, and m_P are the masses of the entire spacecraft, the shuttle, and the mast, respectively, and

$$S_0=\int_{m_S}rdm_S+\int_{m_P}pdm_P \quad (3)$$

$\hat{R}_0$ is a unit vector in the direction of R_0 which is

the zero-order perturbed term of R. The tilde over a symbol denotes a skew symmetric matrix derived from the associated vector. C_0 and ω_0 are the perturbed rotation matrix and the perturbed angular velocity of the frame $x_0y_0z_0$ with respect to the inertial frame, respectively. I_0 is the mass moment of inertia matrix about point 0.

The first-order linear perturbation equations, which govern perturbations in the rigid-body motion and the oscillatory deflection of the structure, are expressed in the matrix form

$$M\ddot{x}+(C_d+G)\dot{x}+(K_S+K_{NS})x=F^* \quad (4)$$

where M, C_d, G, K_S and K_{NS} are mass, damping, gyroscopic, stiffness and stiffening matrices respectively.

$$x^T=[R_1^T,\ \beta^T,\ q^T] \quad (5)$$

$$F^{*T}=[F_1^T,\ M_1^T,\ Q_0^T+Q_1^T] \quad (6)$$

where the first-order perturbed term R_1 of R is a vector measured with respect to axes $x_0y_0z_0$. In order to express all the variables in the perturbation equations in terms of components along the $x_0y_0z_0$ axes, small angular displacement β expressed in the body-fixed frame are introduced. q is a vector of time-dependent generalized coordinates. Q_0 is the first-order perturbed force for elastic displacement. F_1, M_1 and Q_1 are vectors of external forces associated with the perturbations in the rigid-body translations, rigid-body rotations, and elastic displacements, respectively.

2.1 Reduced state equation by Krylov vectors

The order of the perturbation equations for the deflection control is often so large that some reduction is necessary. In the paper, the elastic motion can be expanded into a series composed of premaneuver eigenvectors acting as admissible vectors. Note that the premaneuver eigenvectors can be obtained in a state of equilibrium prior to the maneuver, which may be characterized by either rest or steady rotation. The SCOLE model is reduced by using the frequency dependent Krylov vectors (FDKV) (Sung and Park, 1999a) that demonstrated better dynamic accuracy than the eigenvectors. The equations of motion transformed by FDKV are simplified and their number is significantly smaller than the number of equations in Eq. (4) even if these admissible vectors clearly do not decouple the equations of motion. Using the FDKV, the linear transformation between physical $x^{n\times 1}$ and Krylov $\tilde{z}^{p\times 1}$ coordinates can be considered as

$$x(t)=Q\tilde{z}(t) \quad (7)$$

where $p\leq n$. Hence, the equations of motion in Krylov space are as follows:

$$\begin{aligned}&\bar{M}\ddot{\tilde{z}}(t)+(\bar{C}_d+\bar{G}(t))\dot{\tilde{z}}(t)\\&\quad+(\bar{K}_0+\bar{K}_t(t))\tilde{z}(t)=Q^TF^*(t)\end{aligned} \quad (8)$$

where

$$\begin{aligned}\bar{M}&=Q^TMQ\\ \bar{G}&=Q^TGQ\\ \bar{C}_d&=Q^TC_dQ\\ \bar{K}_0&=Q^TK_sQ\\ \bar{K}_t&=Q^TK_{ns}Q\end{aligned} \quad (9)$$

The reduced equations are called *quasi-Krylov* equations of motion} which are used for computer simulation and deflection control.

All these operations with admissible vectors are guided by the results of a perturbation method such that the nonlinear terms which are functions of both rigid-body angular velocity and angular acceleration, appear in the coefficients of the system matrices.

The quasi-Krylov equations of motion of Eq. (8) could be expressed as a state equation with stochastic effects:

$$\dot{z}(t)=Az(t)+Bu(t)+D(t)+w(t) \quad (10)$$

where

$$A=\begin{bmatrix}0 & I\\ -\bar{M}^{-1}\bar{K} & -\bar{M}^{-1}C_d\end{bmatrix}$$

$$B=\begin{bmatrix}0\\ \bar{M}^{-1}Q^T\end{bmatrix}$$

$$D=\begin{bmatrix}0\\ -\bar{M}^{-1}\bar{K}_t(t)\tilde{z}-\bar{M}^{-1}\bar{G}(t)\dot{\tilde{z}}\end{bmatrix}$$

and the control input and state vector are expressed as $u(t)=F^*$ and $z(t)=\{\tilde{z},\ \dot{\tilde{z}}\}^T$, respectively. The output equation could be expressed as

$$y(t)=Cz(t)+v(t) \quad (11)$$

where state vector $z(t)\in\mathbf{R}^k$, sensor noise vector v

$(t)\in\mathbf{R}^m$, and output vector $y(t)\in\mathbf{R}^l$ are expressed. $D(t)$ contains known disturbances which can be nonlinear time variant functions. Note that the time variant terms decrease in magnitude and the equation approaches a decoupled form as the maneuver velocity decreases.

The plant disturbance vector $w(t)$ and the sensor noise vector $v(t)$ contain independent white-noise processes with zero mean as their elements. Their covariance matrices are given as

$$\mathbf{E}[w(t)w(\tau)^T]=Q_p\delta(t-\tau) \tag{12}$$

$$\mathbf{E}[v(t)v(\tau)^T]=Q_m\delta(t-\tau) \tag{13}$$

where $\delta(t-\tau)$ is the Dirac delta function.

2.2 Elastic tracking model

For the linear motion of a control system, an ideal tracking model is presented to generate desired elastic states so that the natural deflection of a system is experienced. The tracking model is starting with the partition of system matrices. Since the quasi-Krylov equations of motion preserves the physical coordinate information, the reduced equations of motion can be partitioned into two subsystems, such as a rigid-body subplant and a flexible-body subplant by multiplying the inversion of mass matrix $\bar{M}$ to each term with the exclusion of time-varying matrices of Eq. (8)

$$\begin{Bmatrix}\ddot{\bar{z}}_r\\ \ddot{\bar{z}}_f\end{Bmatrix}+\begin{bmatrix}C_{rr} & C_{rf}\\ C_{fr} & C_{ff}\end{bmatrix}\begin{Bmatrix}\dot{\bar{z}}_r\\ \dot{\bar{z}}_f\end{Bmatrix}+\begin{bmatrix}K_{rr} & K_{rf}\\ K_{fr} & K_{ff}\end{bmatrix}\begin{Bmatrix}\bar{z}_r\\ \bar{z}_f\end{Bmatrix}=\begin{Bmatrix}F_r\\ F_f\end{Bmatrix} \tag{14}$$

where the subscripts r and f stand for rigid-body and flexible-body, respectively. From the left side of Eq. (14), the second matrix is the partitioned damping matrix of $C_d=\bar{M}^{-1}\bar{C}_d$ and the third matrix is the partitioned stiffness matrix of $K_0=\bar{M}^{-1}\bar{K}_0$. External loads F_r and F_f are related to rigid-body and to flexible-body, respectively. Note that the mass matrix has been simplified to the identity matrix to conveniently cast Eq. (14) in state space form. The flexible-body, for which the state estimator is designed with the assumption of the direct measurement of the rigid-body states, is

$$\ddot{\bar{z}}_f+C_{ff}\dot{\bar{z}}_f+K_{ff}\bar{z}_f=F_f-D_s(\bar{z}_r,\ \bar{z}_f,\ \dot{\bar{z}}_r,\ \dot{\bar{z}}_f) \tag{15}$$

where $D_s(\bar{z}_r,\ \bar{z}_f,\ \dot{\bar{z}}_r,\ \dot{\bar{z}}_f)$ is considered as a disturbance term including stiffening, gyroscopic, and coupled terms. The Eq. (15) could be efficiently used for the flexible-body state estimation as well as an ideal tracking model.

The tracking model could be obtained from Eq. (15) by excluding time-varying matrices and internal forces so that the tracking model provides ideal elastic states to a controller. It serves as a nominal linear trajectory for a flexible-body dynamics. Using the modal analysis of the partitioned subplant, the transformation between the tracking model and the partitioned model is obtained by

$$\bar{z}_f(t)=Tz_d(t) \tag{16}$$

where $T\in\mathbf{R}^{(k-6)\times(k-6)}$ is an set of eigenvectors of the partitioned model. The tracking model is expressed as

$$\ddot{z}_d(t)+2\zeta\omega_n\dot{z}_d(t)+\omega_n^2z_d(t)=-\mu T^{-1}A_e\ddot{\theta} \tag{17}$$

where A_e is defined as an influence matrix obtained by the terms of Eq. (15) associated with $\ddot{\theta}$ which will be the designed angular acceleration in numerical evaluation. The ζ and ω_n are the damping coefficient and the natural frequency of the partitioned subplant, respectively. Hence, the right hand side (Swigert, 1980) of the Eq. (17) is accounted for a tangential force associated with the desired angular displacement. The μ is a scaling factor which can be used in the case of a high angular velocity maneuver in order to operate the system within either an elastic range or a small deflection. The tracking model of Eq. (17) is employed for the generations of the desired elastic states and a linear guidance.

3. Start-Coast-Stop Maneuver

In reference (Meirovitch and Quinn, 1987b), the perturbation method permits the maneuver strategy to be designed independently of deflection control. In the rigid-body like maneuver with the zero-order perturbation, the axis of rotation is not necessarily a principal axis so that the each moment along the $x_0y_0z_0$ axes of the

zero-order perturbed moment M_0 desired to produce a rigid-body rotation about one axis are obtained as

$$M_{01}=I_{11}\ddot{\theta} \tag{18}$$

$$M_{02}=I_{21}\ddot{\theta}-I_{31}\dot{\theta}^2 \tag{19}$$

$$M_{03}=I_{31}\ddot{\theta}+I_{21}\dot{\theta}^2 \tag{20}$$

where θ is the desired angular displacement. The inertia moments in the above equations are the elements of I_0, the mass moment of inertia, about the rotational axis. These moments are applied to the SCOLE to perform the slewing maneuver with respect to one axis.

For the rest-to-rest roll maneuver, there are several operational strategies (Farrenkopf, 1979, Junkins and Turner, 1986, Swigert, 1980) devised by optimal formulation in order to minimize either operational time or fuel, or both of them, which lead to solutions for two-point boundary value problems. Instead of the complicated formulation, a simple operation is employed and targeted to the reduction of both operational time and fuel consumption. A torque command input $M_{01}=u_c(t)$ for roll maneuver around x_0 axis in the paper used in conjunction with the input shaping technique is expressed as

$$u_c(t)=T_{amp}\sin^2\Omega t,\ t\le t_0=\frac{\pi}{\Omega} \tag{21}$$

$$u_c(t)=0,\ \textit{otherwise}$$

where T_{amp} is the torque magnitude and Ω is the period of torque input profile. The input profile is used for start and stop motions. During the coasting period, no additional input is required except for control input to treat disturbances. The smooth input profile is selected because the excitation of high frequency modes should be reduced during the transient period.

In order to accurately arrive at the desired final angle of the roll maneuver, an analytical solution for intermediate time interval is needed. By taking time integration of Eq. (18) with Eq. (21), the desired coasting angular velocity is given as

$$\dot{\theta}_c=\frac{T_{amp}}{I_{11}}\left(\frac{t_0}{2}-\frac{sin2t_0}{4}\right) \tag{22}$$

where $\dot{\theta}_c$ is the costing angular velocity of $\dot{\theta}$. If the desired final angle θ_f is given, the coasting time interval, t_c, can be obtained as

$$t_c=t_0+\frac{\theta_f}{\dot{\theta}_c} \tag{23}$$

4. Numerical Simulation to SCOLE Model

The finite element model of the SCOLE in Fig. 1 presented by Meirovitch and Quinn (1987b). The mast supporting the antenna is a steel tube 10 feet (3.048 m) long. The antenna consists of 12 aluminum tubes, each 2 feet (0.6096 m) long, welded together to form a hexagonal-shaped grid. The shuttle is simulated by a steel plate of uniform thickness with a mass of 13.85 *slugs* (202.1241 Kg_m). The material and physical properties can be found in reference (Meirovitch and Quinn, 1987a). All computations were performed on an IBM RISC 6000 Workstation. The control schematic diagram is shown in Fig. 2. There are 3 torque and 3 force actuators applied for the maneuver and control of the shuttle. 3 torque wheels are mounted at the mast-tip to control structural deflection. For state estimation, it is assumed that the ω_0, R_0, and $\dot{R}_0$ of the shuttle can be measured with respect to the inertial frame XYZ. The state variables of the mast relative to $x_0y_0z_0$ are estimated by the Kalman filter using 3 displacement (x, y, and z) and 3 velocity ($\dot{x}$, $\dot{y}$, and $\dot{z}$) sensors mounted at the mast-tip. The configuration of the actuators and sensors is collocated at both the shuttle and the mast-tip.

The full-order model, 84 degrees of freedom, is reduced to 12 degrees of freedom by configuring two pseudo-actuators at the mast-tip in the x and y directions and two pseudo-sensors at the same locations and directions as the two actuators in

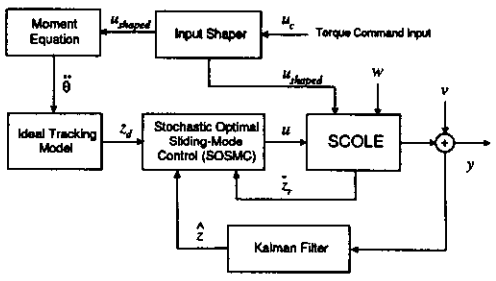

Fig. 2 Schematic control diagram

Table 1 Design parameters for controller and estimator

Rigid-body feedback coefficient	$\varkappa$	1000
Global reaching coefficient	ν	20
Scaling factor	μ	1
Influence matrix	A_e	$I^{(k-6)\times(k-6)}$
Rigid-body weighting	Q_p	$10^{-3}I^{(k-6)\times(k-6)}$ meter
Measurement noise intensity	Q_m	$10^{-4}I^{(k-6)\times(k-6)}$ meter
Open loop torque period	Ω	4.0 rad/sec

the application of the frequency dependent Krylov sequence (FDKV) (Sung and Park, 1999a). The configuration is reflected by the true locations of actuators and sensors in controlling the deflection of the mast. The 6 elastic modes of the 12 mode FDKV model are obtained from the first 2 vectors with $\sigma_r=55$ rad/sec and the last 4 vectors with $\sigma_f=10$ rad/sec. The damping formula is written as $C_d=\alpha M+\beta K$ where $\alpha=\beta=0.01$ were selected. A more detailed description of the FDKV algorithm is provided in the reference (Sung and Park, 1999a) for the multidimensionality and collocation of actuators and sensors and the selection of starting vectors.

Initially, the SOSMC (Sung, 1997) was developed to control the oscillatory deflection of a large flexible structure with the least chattering effect and the globally asymptotic stability. The control law is, mainly, composed of the sliding-mode control and the Kalman filtering to implement a boundary feedback control. For the flexibility control and the large angle rigid-body maneuver of a spacecraft, the SOSMC law could be modified and expressed as

$$\begin{aligned} u(t)=&-(G_cB)^{-1}[G_c(A-K_fC)z_e(t)\\ &+P_sG_cz_e(t)+\varkappa G_cz_{re}(t)+G_cK_fy(t)\\ &+G_cD(t)-G_c\dot{z}_d(t)] \end{aligned} \tag{24}$$

where an attitude error feedback term $\varkappa G_cz_{re}(t)$ is introduced to control the shuttle. G_c is a sliding surface gain matrix. The $D(t)$ contains known nonlinear functions which can be obtained from the mathematical model of the SCOLE. $z_{re}(t)$ is only the rigid-body state error obtained from Eqs. (14), (18), (19) and (20). $z_e(t)=\hat{z}(t)-z_d(t)$ is the state error where $\hat{z}(t)$ and $z_d(t)$ are estimated state and desired state vectors, respectively. K_f is a time-varying Kalman filter gain matrix. A diagonal matrix $P_s=\nu I^{m\times m}$ is selected for a globally asymptotic sliding surface. Several design parameters are tabulated in Table 1.

In the numerical simulation, four cases are compared with respect to the antenna rotations. The four cases are

1. *Tracking Control (a)* requires that most nonideal effects are assumed to be known for the design of the SOSMC and time-varying Kalman filter. However, the SOSMC does not include the time-varying effects such as stiffening and gyroscopic terms. The SOSMC attempts to follow the states of the ideal tracking model. The control efficiency is demonstrated by this case.

2. *Tracking Control (b)* allows the most significant disturbances in the slewing maneuver to be dropped in the design of the SOSMC and time-varying Kalman filter out of the *Tracking Control (a)* case. The disturbances are the tangential and centrifugal forces. The SOSMC again tracks the states of the ideal tracking model. The robustness of the SOSMC is illustrated by this case.

3. *Open-Loop Control* in that neither the SOSMC nor Kalman filter is involved. The input shaping technique is used to evaluate the performance with only two-impulse sequence.

4. *Rigid-Body Control* in that the ideal tracking model is not used. The SOSMC is attempting to hold the flexible mast like a rigid-body.

In the four cases, the input torque command u_{shaped} with the magnitude $T_{amp}=20$ $ft\cdot lb_f$(2.7651 $Kg_f\cdot m$) in Fig. 3 is shaped by a two-impulse sequence (Singer, 1989) with respect to the first mode of the tracking model and then is applied to the shuttle for a 30° roll maneuver. The tracking model generates four non-zero states and maintain the remaining states at zero. The stochastic optimal sliding-mode controller is char-

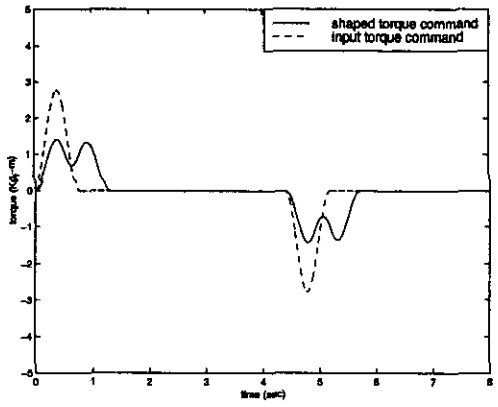

Fig. 3 Shaped and unshaped command inputs for 30° roll maneuver

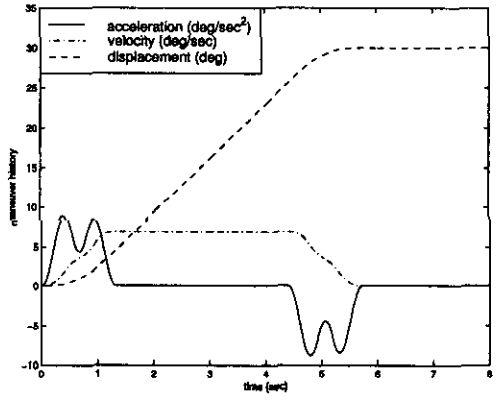

Fig. 4 Maneuver strategy for 30° roll maneuver

ged with rejecting perturbations during the entire slewing motion. The desired motion of the shuttle is shown in Fig. 4 with the maximum velocity around 6 deg/sec.

The main control objective of the SCOLE model is to aim the antenna within the certain tolerance 0.02° in a short time. Hence, a study of the antenna rotations versus time is of interest.

Figures 5 to 7 illustrate the instantaneous antenna rotations with respect to $x_0y_0z_0$ about the x_0, y_0 and z_0 axes, respectively. The figures show the responses produced during the maneuver with all four of the control techniques. The effect of the tangential and centrifugal terms in the controller and estimator in the case of tracking control (b) shows more angular displacement and takes a longer time than the one of tracking control (a) to settle down the oscillatory rotation because the

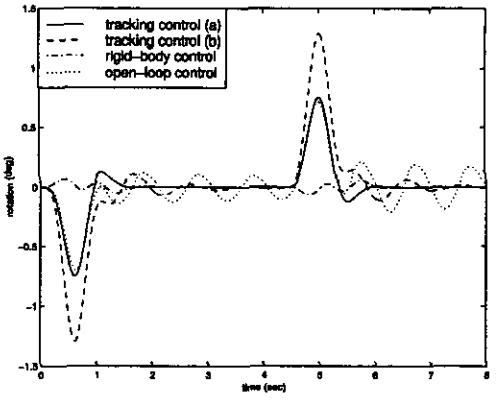

Fig. 5 Antenna rotation about x_0 during a 30° roll maneuver

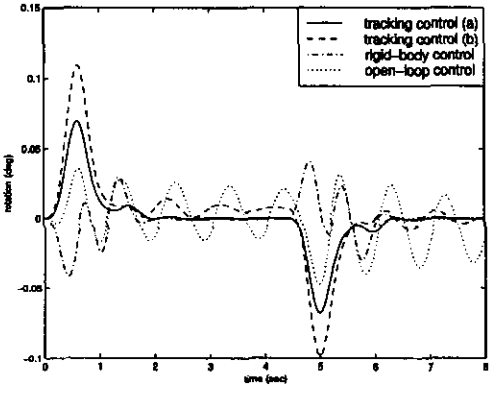

Fig. 6 Antenna rotation about y_0 during a 30° roll maneuver

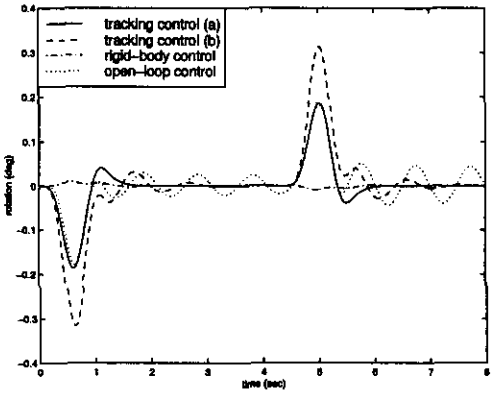

Fig. 7 Antenna rotation about z_0 during a 30° roll maneuver

SOSMC is employing a globally asymptotic reaching technique (Mostafa and Öz, 1989) unlike a rapid switching technique. Nevertheless, it does

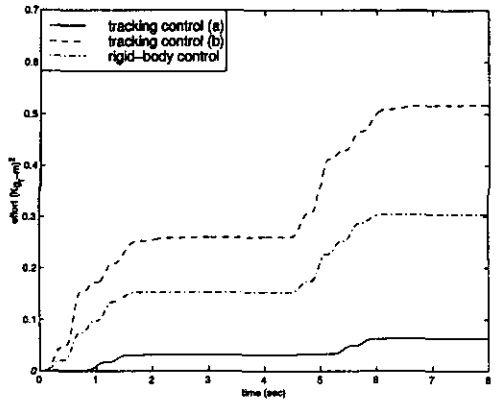

Fig. 8 Torque control efforts during a 30° roll maneuver

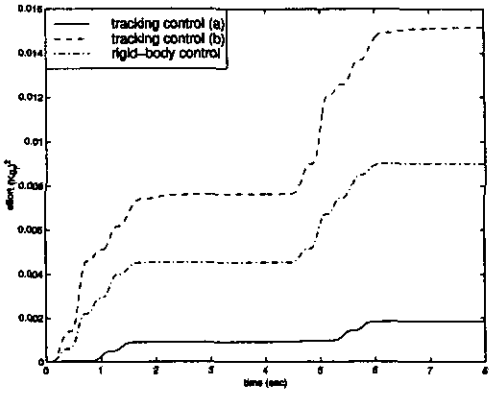

Fig. 9 Force control efforts during a 30° roll maneuver

eventually and quickly damp out the residual oscillatory rotational deflection of all axes in the presence of modeling errors in the tracking control (a) which is performed within settling time 0. 25 sec at the target angle 30°. The open-loop case with input shaping alone can not reach the design tolerance and shows continuous rotational displacement. The rigid-body maneuver case shows a lot of rotational displacement during maneuver and longer settling time than the proposed one.

The measure of economical control effort ($C.E.$) is defined as

$$C.E.=\int_0^\infty u(t)^T u(t)dt \tag{25}$$

The actual control effort is obtained by transforming the Krylov space into the physical coordinate system. In Figs. 8 and 9, the rigid-body control is consuming more control energy in reducing the oscillatory deflection compared to the tracking control (a). The tracking control (b) requires more control effort than the two other cases, and after 6 sec, continuously consumes energy in order to damp out the residual oscillatory deflection. The tracking control (a) consumes the least amount of control effort and accomplishes the 30 ° maneuver so that it is desirable for good control performance to have the precise system modeling. The control effort for the entire system operation in the tracking control (a) is a small quantity below 5 $(ft \cdot lb_f)^2$ (0.4781 $(\mathrm{Kg}_f \cdot \mathrm{m})^2$) which can be indirectly comparable to the results of Meirovitch and Quinn (1987b). They used either distributed force actuators or 10 discrete force actuators in controlling the oscillatory deflection of the mast instead of using torque wheel actuators in the paper.

5. Conclusion

For the large slewing maneuver of a flexible spacecraft, a robust control mechanism was proposed and evaluated with an application to the SCOLE by composing the SOSMC, an elastic tracking model and the command shaping technique with a start-coast-stop maneuver. In order to reduce the rotational deflection and perform efficient operation of the flexible spacecraft, the SCOLE model is reduced by the FDKV algorithm to release a computational burden. The proposed robust control approach was shown to be more energy efficient than the rigid-body motion maneuver's. The control robustness was demonstrated by neglecting the most significant disturbances without instability issues. As a result, the large slewing maneuver is successfully accomplished without significant residual rotational deflection in a relatively short period of time when pointing the antenna to a different target in a space environment.

References

Farrenkopf, R. L., 1979, "Optimal Open-Loop

Maneuver Profiles for Flexible Spacecraft," *Journal of Guidance, Control, and Dynamics*, Vol. 2, No. 6, pp. 491~498.

Gupta, N. K., 1980, "Frequency-Shaped Cost Functionals: Extension of Linear-Quadratic-Gaussian Design Methods," *Journal of Guidance, Control, and Dynamics*, Vol. 3, No. 6, pp. 529~535.

Junkins, J. L. and Turner, J. D., 1986, *Optimal Spacecraft Rotational Maneuvers*, Elsevier Science Publishers, New York.

Meirovitch, L. and Quinn, R. D., 1987a, "Maneuvering and Vibration Control of Flexible Spacecraft," *Journal of the Astronautical Sciences*, Vol. 35, No. 3, pp. 301~328.

Meirovitch, L. and Quinn, R. D., 1987b, "Equation of Motion for Maneuvering Flexible Spacecraft," *Journal of Guidance, Control, and Dynamics*, Vol. 10, No. 5, pp. 453~465.

Mostafa, O. and Öz, H., 1989, "Chatter Elimination in Variable Structure Control Maneuvering of Flexible Spacecraft," *Journal of the Astronautical Sciences*, Vol. 37, No. 4, pp. 529~550.

Singer, N. C., 1989, "Residual Vibration Reduction in Computer Controlled Machines," Ph. D Thesis, Massachusetts Institute of Technology.

Sinha, A. and Miller, D. W., 1995, "Optimal Sliding-Mode Control of a Flexible Spacecraft under Stochastic Disturbance," *Journal of Guidance, Control, and Dynamics*, Vol. 18, No. 3, pp. 486~492.

Slotine, J-J. E., 1985, "The Robust Control of Robot Manipulators," *Journal of Robotics Research*, Vol. 4, No. 2, pp. 49~64.

Sung, Y-G, 1997, "Model Reduction and Robust Vibration Control of Large Flexible Space Structures," Ph. D. Thesis, The University of Alabama, Tuscaloosa, Alabama.

Sung, Y. -G. and Park, Y. -P., 1999a. "Model Reduction of Semi-Positive Definite Systems Reflected to Actuator and Sensor Locations," *KSME International Journal*, Vol. 13, No. 10, pp. 714~726.

Sung, Y. -G., 1999b, "Adaptive Robust Vibration Control with Input Shaping as a Flexible Maneuver Strategy," *KSME International Journal*, Vol. 13, No. 11, pp. 807~817.

Swigert, C. J., 1980, "Shaped Torque Technique," *Journal of Guidance, Control, and Dynamics*, Vol. 3, No. 5, pp. 460~467.

Young, K. D. and Öz, U., 1993, "Frequency Shaping Compensator Design for Sliding mode," *Journal of Control*, Vol. 57, No. 5, pp. 1005~1019.